Scaling properties of stretching ridges in a crumpled elastic sheet

Alex Lobkovsky*
Sharon Gentges* Hao Li*§
David Morse‡
T.A. Witten*†

Submitted as a report to *Science*

ABSTRACT

Strong deformation of a sheet of solid material often leads to a crumpled state having sharp points of high curvature. A scaling property governing the crumpled state has been numerically demonstrated by examining the *ridges* joining pairs of sharp points in a range of simple geometries of variable size. As the linear size X increases sufficiently, the deformation energy grows as $X^{1/3}$. Remarkably, it consists of similar amounts of bending and stretching energy. This energy becomes concentrated in a fraction of the sheet that decreases as $X^{-1/3}$. Despite this concentration, the local strain in the ridge decreases, as $X^{-2/3}$. Nearly all the deformation energy in thin, crumpled elastic sheets should be concentrated in ridges that obey these scaling laws.

Buckled sheets such as a crumpled piece of paper, a collapsed storage tank or a shriveled raisin, represent a ubiquitous form of material deformation. These objects may be viewed as thin, elastic sheets that have been strongly deformed by some external force. Such "post-buckling" phenomena have been extensively studied in macroscopic sheets because of their importance for structural failure (1,2) and for cushioning of mechanical impact (3,4). Two features emerge from these studies. First, the deformation appears concentrated around points and

* James Franck Institute, University of Chicago, Chicago IL 60637. internet: `http://arnold.uchicago.edu/MRSEC`

§ Present address: NEC Research Institute, 4 Independence Way, Princeton, NJ 08540.

‡ Institute for Theoretical Physics, University of California, Santa Barbara CA 93106.

† To whom correspondence should be addressed; `internet t-witten@uchicago.edu`.

lines that proliferate with increasing compression, as illustrated in Fig. 1. Second, the compressive force increases smoothly and progressively over a broad range of compression factors (3,5). These same features are expected for microscopic elastic membranes, such as layered compounds (6) (See Fig. 1*c*) and solidlike surfactant vesicles (7).

Current understanding of the strongly buckled state remains primitive. Some scaling properties of this state have been explored empirically (8,9,10). Still, it is not even known how the energy of a crumpled sheet ought to scale with compression. With such scaling laws one could predict for instance the energy of a large crumpled sheet given that of a smaller one. Mathematical treatment of strong buckling has been confined to isolated cases (11,12,13) with different behavior than that of a crumpled sheet. The bulk of analytical work concerns sheets *weakly* deformed by thermal fluctuations (14,15) or by incipient buckling (16,17). Below, we demonstrate a structural element responsible for the deformation energy of strongly buckled thin sheets: the *stretching ridge*.

Fig. 1: Examples of buckled and crumpled sheets. a) simulated buckled thin cylinder, after Ref. 18; b) a piece of paper lightly crumpled between the hands; c) rag phase of molybdenum disulfide after Ref. 19 (calibration bar is 20 nm).

To define this strong buckling, we imagine a thin, flat elastic disk confined in an impenetrable sphere. The thickness h of the disk is taken to be much smaller than its radius R_0 so as to accentuate the contrast with an ordinary three-dimensional solid. The confining sphere is gradually contracted to a radius $R < R_0$, so that the sheet within it must deform. A point originally at spatial position $\vec{s} \equiv (s_1, s_2, 0)$ moves to the point $\vec{r}(\vec{s})$. The deformation energy is the sum of the strain energy S and bending energy B. The sheet takes on a conformation $\vec{r}(\vec{s})$ that minimizes the energy $S + B$.

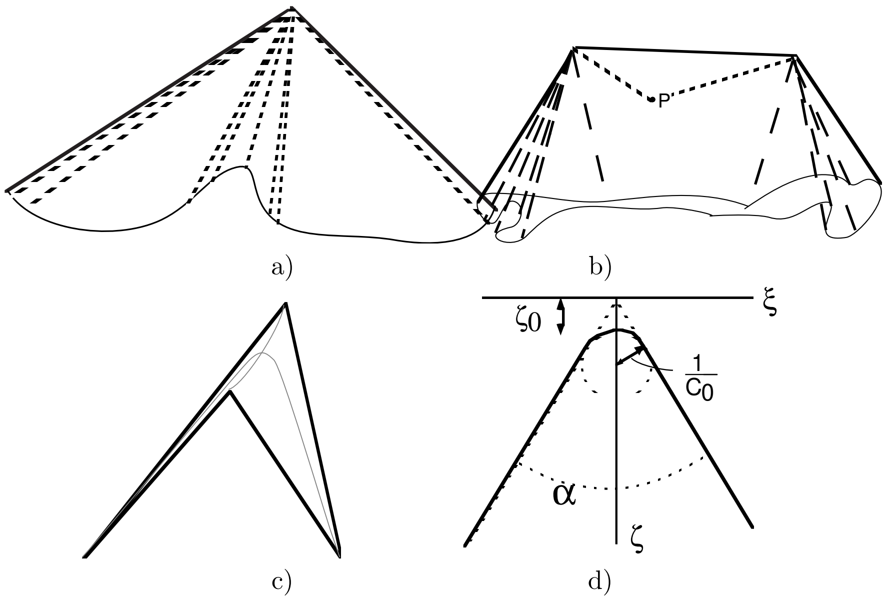

Fig. 2: Deformations of a thin sheet with increasing confinement. a) cone shape resulting from moderate confinement; b) double-cone shape resulting from further confinement. A generic point P is indicated, as discussed in the text. c) schematic view of kite shape discussed in the text. d) approximate shape of the transverse diagonal in c). Axes for normal co-ordinate ζ and transverse co-ordinate ξ are shown. Deflection ζ_0 from unstretchable ridge and dihedral angle α are indicated.

We expect the confined sheet to bend in preference to stretching when $R \gg h$. Accordingly, we first consider an *unstretchable* sheet. Every point on such a sheet must have vanishing curvature in some direction (20). Now if the confining sphere is contracted to, say, two thirds of the radius R_0, the sheet can distort into a conical shape, as shown in Fig. 2*a*, with a singular curvature at the vertex. At each point of the cone there is no curvature in the direction towards the vertex. The radius of curvature $1/C$ grows linearly with distance from the vertex. The resulting energy $B = \kappa \int^{R_0} d^2s\ C^2$ grows logarithmically with the size R_0. Here κ is the cylindrical bending modulus and the integration is taken over the surface (16). As the confining sphere is contracted further, a single cone can no longer fit inside it. An increasing number of singular vertices is necessary. This leads us to investigate the shape of a surface with *two* such

vertices, as sketched in Fig. 2*b*.

The addition of a second vertex alters the curvature qualitatively. A generic point P must now have zero curvature in the direction of both the first vertex and the second. Thus the surface must be *flat* except along the line joining the vertices. This line must form a sharp ridge, whose energy is proportional to its length. The energy increases with the system size R_0 qualitatively more strongly with two vertices than with one. We now allow the surface to stretch. The effect on the single cone is minor: the singularity at the vertex spreads over a finite region whose size is independent of R_0. The case of two vertices was recently discussed elsewhere (21). It was argued that stretching allows the ridge to soften to a radius of curvature $1/C$ of order $h^{1/3} R_0^{2/3}$. The associated energy was argued to grow as $R_0^{1/3}$. For very thin sheets, such an energy would be qualitatively larger than the single-vertex energy, yet qualitatively smaller than the energy of an unstretchable sheet treated above.

We may extend the energy-balance reasoning (21) to treat the ridge joining two vertices, as in the double-cone shape of Fig. 2*b*. We imagine an initial state in which the stretching moduli G are very large and the ridge is a sharp crease of length X, bent through a dihedral angle α, like the kite shape of Fig. 2*c* (22). Now the moduli G are gradually decreased so that stretching is allowed and the transverse curvature at the ridge relaxes, assuming a value C_0 at mid-ridge. We suppose, and later justify, that the bulk of the deformation occurs in a strip along the ridge of width $w \simeq 1/C_0$. Then as C_0 decreases, the strip must deflect away from the original ridge line by an amount ζ_0 of order $1/C_0$. (If the transverse lines were simply rounded at the apex as shown in Fig. 2*d*, then $\zeta_0 = \{[\sin(\alpha/2)]^{-1} - 1\}/C_0$.) The deflection of the strip results in stretching along the ridge: the sheet must be strained by an amount $\gamma \simeq (\zeta_0/X)^2 \simeq (XC_0)^{-2}$. The energy $S = G \int d^2s \gamma^2$ for this stretching of the strip is of order $G\gamma^2 Xw \simeq GX^{-3}C_0^{-5}$. The energy B to bend the strip is of order $\kappa C_0^2 Xw \simeq \kappa X C_0$. To minimize the sum of these two energies requires

$$C_0 \simeq (1/X)\left(X/\sqrt{\kappa/G}\right)^{1/3}.$$

For sheets made of isotropic material the length $\sqrt{\kappa/G}$ is approximately equal to the thickness h (16). The optimal energy achieved is of order $S \simeq B \simeq \kappa(X/h)^{1/3}$.

To reduce the ridge energy further would require deformation in other regions. But the cost of such deformations would outweigh their benefit. Thus to reduce the distance X between the vertices substantially would require a strain of order γ over much of the surface—a region much larger than the ridge. The energy cost would clearly be larger than the ridge energy. Likewise if the flanks of the ridge stretched so as to reduce the needed deflection of the ridge line, the required strain would be of order γ over much of the surface, and the cost would again be prohibitive.

To test these scaling predictions, we have modeled the elastic sheet numerically as a triangular lattice of springs, following for example Seung and Nelson (13,23,24). Some minimum-energy surfaces are shown in Fig. 3. The pictures show a variety of secondary structures near each ridge. The stretching energy oscillates as one moves away from the ridge line of the tetrahedron rather than going monotonically to zero. For the shapes with a free edge (Figs. 3c and 3d), there are regions of large curvature at the free edge opposite to the vertices. Faint induced ridges appear between the vertices and the induced "vertices" at the edges. These induced features become stronger as the effective size X/h increases.

In Fig. 4 we plot the transverse curvature at mid-ridge *vs.* the reduced size X/h for the four different shapes. The curvature is expressed relative to the curvature at the same point if only one vertex were present. We note first that the curvatures follow the anticipated $(X/h)^{1/3}$ scaling. The tetrahedron has a reduced curvature of $0.22(X/h)^{1/3}$, as determined from fitting all the data. The uncertainty in this coefficient derived from the scatter of the data is less than 0.001. Second, the curves for different shapes have similar slopes. This indicates that the shape of the ridge does not depend strongly on the sharpness of the vertices or on the shape of the surface far from the ridge. Third, the dihedral angle α affects the slope more than the sharpness of the vertices does. For the bag shapes (Fig. 3*c*), with fixed sharpness, the slope increases with the bag length (that is, with decreasing α). But for different shapes with equal dihedral angle (Figs. 3a and 3b), there is no discernable difference in slope. Fourth, in all cases, the ridge begins to dominate the curvature (doubling the reduced curvature) for X/h in the range of 350 to 1000.

We analyzed the tetrahedral shape in greater detail. We first verified that the shapes were independent of lattice size for fixed X/h. The curvature at mid-ridge differs from the extrapolation to an infinitely fine lattice by no more than two percent. The entire profile shrinks inward with increasing X/h; the shrinkage is consistent with the anticipated $(X/h)^{-1/3}$ scaling. This can be seen by plotting the mean-squared curvature across the ridge as shown in the inset of Fig. 4 for four different X/h's. The ridge profiles collapse onto a single scaling curve. Since our results are insensitive to the lattice spacing for a given X/h, they are not sensitive to the lattice spring model used, but would hold quantitatively for any elastic material.

The total energy of the tetrahedron is expected to scale as $\kappa(X/h)^{1/3}$. In Fig. 5 we plot the measured total energy $S + B$ in units of κ. The energy is

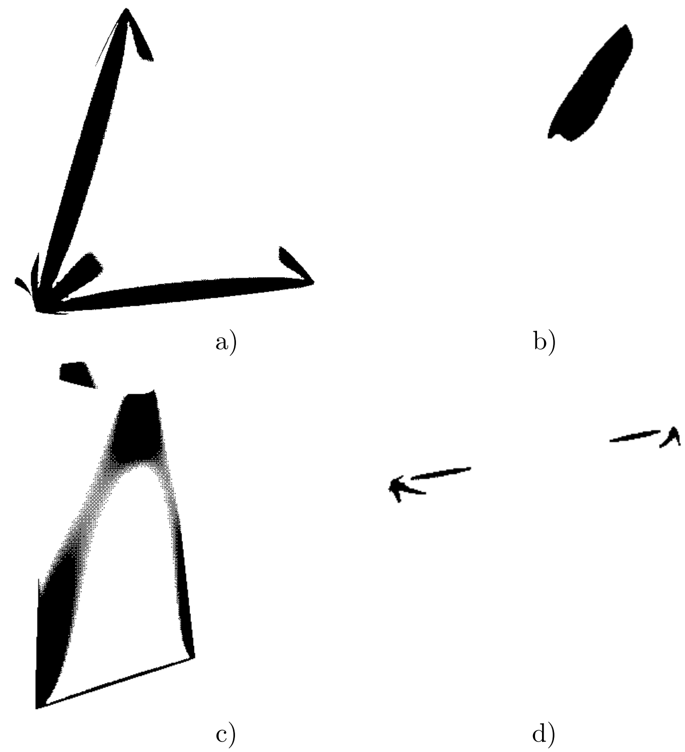

Fig. 3: Sample shapes simulated in the present study using a triangular lattice of springs of unstretched length a and spring constant K. Shading is proportional to local stretching energy. Bending rigidity is imparted by an additional energy $J(1 - \hat{n}_i \cdot \hat{n}_j)$ for each pair of adjacent triangles (i, j) with unit normals $\hat{n}_i$ and $\hat{n}_j$ (13). This lattice is equivalent to a sheet of isotropic elastic material of thickness $h = 2\sqrt{2}\sqrt{J/K}$ and bending modulus $\kappa = \sqrt{3}/2\ J$. a) regular tetrahedron. Distance X between vertices is 100 times the lattice spacing a. Elastic thickness $h = a/27.4$. b) kite shape made from a flat, rhombus-shaped surface by exerting normal forces on the perimeter sites. The forces constrain the perimeter to follow a rectilinear frame with dihedral angle α equal to that of the tetrahedron, namely $\cos^{-1}(1/3)$. Ridge length $X = 100a$ and thickness $h = a/13.7$. c) two-vertex bag shape with $X = 50a$, $h = a/27.4$, and length of $2X$. "Sharpness" of vertices (integrated gaussian curvature or disclination charge) is π as in a regular tetrahedron. d) two-vertex boat shape with $X = 67.48a$ and $h = a/20.4$. The two vertices have sharpness $\pi/3$.

consistent with the asymptotic formula $S + B = 6\kappa(1.55 \pm .002)(X/h)^{1/3}$. The

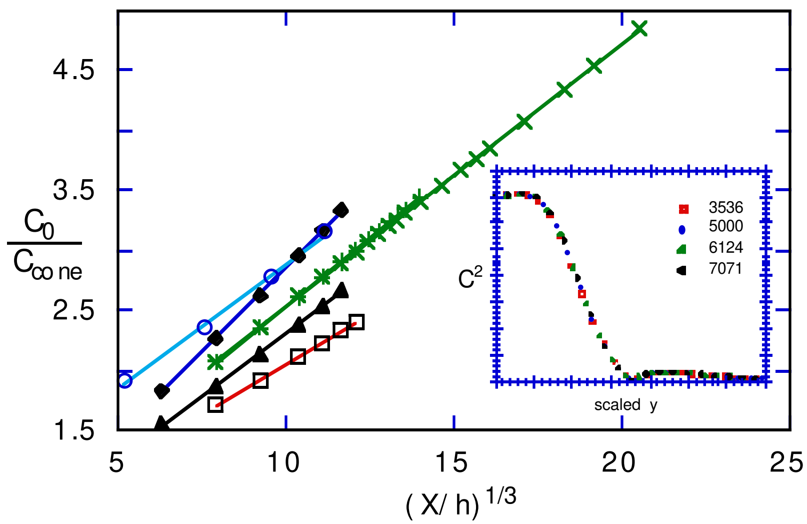

Fig. 4: Midridge curvatures for simulated surfaces, relative to the curvature of a single cone at the same distance from its vertex. Horizontal axis is the anticipated scaling variable $(X/h)^{1/3}$. open squares, kite shapes; open circles, boat shapes; closed triangles, bags of length X; closed diamonds, bags of length $2X$; plusses, tetrahedrons with ridge length $X = 50a$; x's, tetrahedrons with ridge length $X = 100a$. Straight lines indicate the anticipated scaling behavior. Inset: mean-squared local curvature C^2 scaled by $X^{-2}(X/h)^{2/3}$ along the perpendicular bisector of the ridge. The distance y from the ridge is scaled by $X(X/h)^{-1/3}$ for tetrahedron ridges with different X/h as indicated. Strain profile $\gamma(y)$ is similar.

indicated uncertainty reflects only the scatter in the data used. For comparison we show the combined energy of the four disconnected cones making up the tetrahedron, namely

$$4\kappa(4.081 \log(X/a) + \text{const.}). \tag{6}$$

The cone energy is independent of the moduli G and thus independent of the elastic thickness h (25). Evidently the cone energy remains a significant fraction of the tetrahedron energy for all tetrahedra studied. Nevertheless the asymptotic scaling gives less than ten percent error for tetrahedra larger than about 10^3 times their thickness (For example a ten-centimeter tetrahedron made of standard tenth-millimeter-thick office paper). The simulated sheets of Tersoff

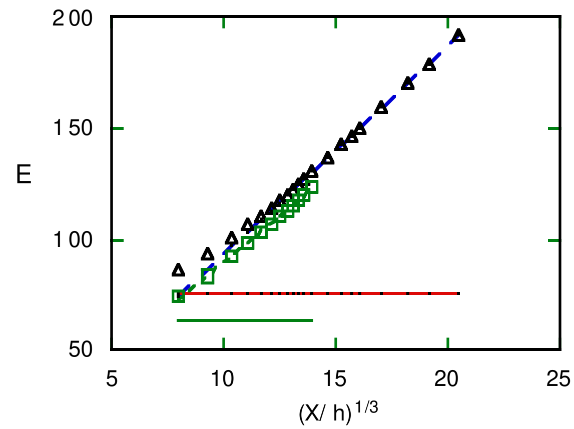

Fig. 5: Total energy $E = S + B$ in units of bending modulus κ for lattice tetrahedra with $X = 50$ lattice units (squares) and 100 lattice units (triangles), *vs.* $(X/h)^{1/3}$. Dashed lines: least-square fits through upper seven points of the data. Solid lines: continuum energies of four separated cones with sharpness π as in a tetrahedron and with length X, using Eq. 6 without the additive constant. lower line: $X = 50$ lattice units; upper line: $X = 100$ lattice units. (Numerically-determined cone energies fall close to these lines.)

(26) and of Kroll (24) did not approach these size-to-thickness ratios. Thus it is not surprising that they saw no evidence for the energy scaling predicted here.

The ridges suggest an approach for describing a strongly crumpled sheet. By common observation, crumpled sheets contain a large number of vertices. We may suppose that pairs of adjacent vertices give rise to ridges like the ones seen in our simple shapes. The neighboring ridges can be expected to influence one another. Still, this mutual influence cannot be too great. Our study has shown that well-developed ridges are but little influenced by the surface at distances of order X from the ridge line. This is natural, since the ridge energy is concentrated at distances much smaller than X from this line. We are led to treat the ridges as independent, at least as a first approximation. Thus, we may find the approximate energy of a given crumpled sheet from its ridge lengths X_i by simply adding the individual energies to obtain a total energy $E \sim \sum_i (X_i)^{1/3}$.

We expect the stretching-ridge concept to contribute significantly to future understanding of the crumpled materials like those pictured in Fig. 1. For ridges longer than a few hundred times the membrane thickness, the ridges give a *quantitative* account of the deformation energy. The ridge concept should aid in the design of macroscopic energy-absorbing materials like packing material (4) and protective vehicle structures (3), for example by placing defects to control where ridges form. Ridges may aid the understanding of microscopic phenomena like the collapse of graphite membranes (6) and the passage of blood cells through capillaries (27). And they may elucidate large-scale phenomena like the buckling of the earth's crust (28).

REFERENCES AND NOTES

1. *Post-buckling of elastic structures*, proceedings of the Euromech Colloquium, no. 200, Matrafured, Hungary, 5-7 October 1985 (Elsevier, Amsterdam 1986).
2. N. Yamaki, *Elasic Stability of Circular Cylindrical Shells* (Horth-Holland, New York 1984).
3. P. Stutenkemper and R. Brasche, in *International Technical Conference on Experimental Safety Vehicles* Paris, June 1979 (U.S. Govt. Printing Off., Washington DC, 1980)
4. C.E. Crede, in *Symposium on Simulated Service Testing of Packging* New York NY, 1962 (ASTM, Philadelphia, 1963)
5. R. E. Newton, in *Shock and Vibration Handbook* C. M. Harris and C. E. Crede, Eds. (McGraw-Hill, New York, 1988), p. 31-1; P. E. Franklin and M. T. Hatae, *ibid* p. 41-1.
6. M. S. Spector, E. Naranjo, S. Chiruvolu, J. A. Zasadzinski, *Phys. Rev. Letts.*, **73** 2867 (1994)
7. E. Sackmann, P. Eggl, C. Fahn, H. Bader, H. Ringsdorf, M. Schollmeier *Ber. Bunsenges. Phys. Chem.* **89** 1198 (1985).
8. J.B.C. Garcia, M.A.F. Gomes, T.I. Jyh, and T.I. Ren, *J. Phys A.* **25**, L353 (1992).
9. F. Abraham, paper presented at Workshop on Biomaterials, University of California, Santa Barbara, CA, 31 August 1994.
10. Y. Kantor, M. Kardar, D. R. Nelson, *Phys. Rev. Lett.* **57** 791 (1986).
11. R. Scheidl and H. Troger , in Ref. 1, p. 293.
12. Michael Ortiz and Gustavo Giola, *J. Mech. Phys. Solids* **41** 531 (1994).
13. H. S. Seung and D. R. Nelson, *Phys. Rev. A* **38** 1005 (1988).
14. See *Statistical Mechanics of Membranes and Surfaces* D. Nelson, T. Piran, and S. Weinberg, Eds., World Scientific (1989).
15. D. R. Nelson and L. Peliti *J. Phys. (Paris)* **48** 1085 (1987); F. David and E. Guitter, *Europhys. Lett.* **5** 709 (1988).
16. L. D. Landau and E. M. Lifshitz, *Theory of Elasticity* (Pergamon, Oxford, 1986), Sections 14 and 15. Our cylindrical bending modulus κ is denoted there as D.

17. See for example George Gerard, *Handbook of structural stability* (New York University, New York NY, 1956).
18. Yannick L. Kergosien, Hironobu Gotoda, and Tosiyasu L. Kunii, *IEEE Computer Graphics and Applications*, **14** 40 (1994).
19. R. R. Chianelli, E. B. Prestridge, T. A. Pecoraro and J. P. DeNeufville, *Science* **203** 1105 (1979).
20. Ref. 14, p. 143.
21. T. A. Witten and H. Li *Europhysics Letters* **23** 51 (1993).
22. Full description requires two stretching and two bending moduli; however, these details are not important for our scaling argument.
23. D.C. Morse, and T.C. Lubensky *Journal de Physique II* **3** 531 (1993).
24. Z. Zhang, H. T. Davis, D. M. Kroll, *Zeitschrift fur Physik. B, Condensed matter* **97** 337 (1995).
25. More precisely, the cone energy is independent of h in the limit that h is much smaller than the lattice spacing a. In our numerical studies h varied from a to a few percent of a. Accordingly, we observed a few-percent dependence of the cone energy on h.
26. J. Tersoff *Phys. Rev. B* **46** 15546 (1992).
27. W. H. Reinhart, *et al.* *Biorheology* **28** 537 (1991).
28. See. for example R. J. Chorley, S. A. Schumm, D. E. Sugden, *Geomorphology* (Methuen, London, 1984), Chapter 7.

29. The authors are grateful to J. Gao, N. Lebovitz, S. Antman and S. Nagel for assistance and discussions. This research was supported the US National Science Foundation under Award number DMR-9205827 and through its MRSEC Program under Award number DMR-9400379. S. G. was supported as a summer intern by the National Science Foundation Research Experiences for Undergraduate Program under NSF REU Site Grant Phy-9212351. We thank the authors of Ref. 18 for providing the image for Fig. 1*a*.